

Lighting Up the Force: Investigating Mechanisms of Mechanotransduction Using Fluorescent Tension Probes

Carol Jurchenko, Khalid S. Salaita

Department of Chemistry, Emory University, Atlanta, Georgia, USA

The ability of cells to sense the physical nature of their surroundings is critical to the survival of multicellular organisms. Cellular response to physical cues from adjacent cells and the extracellular matrix leads to a dynamic cycle in which cells respond by remodeling their local microenvironment, fine-tuning cell stiffness, polarity, and shape. Mechanical regulation is important in cellular development, normal morphogenesis, and wound healing. The mechanisms by which these finely balanced mechanotransduction events occur, however, are not well understood. In large part, this is due to the limited availability of tools to study molecular mechanotransduction events in live cells. Several classes of molecular tension probes have been recently developed which are rapidly transforming the study of mechanotransduction. Molecular tension probes are primarily based on fluorescence resonance energy transfer (FRET) and report on piconewton scale tension events in live cells. In this minireview, we describe the two main classes of tension probes, genetically encoded tension sensors and immobilized tension sensors, and discuss the advantages and limitations of each type. We discuss future opportunities to address major biological questions and outline the challenges facing the next generation of molecular tension probes.

Multicellular organisms depend on the ability of individual cells to communicate with each other and sense their external environment, including the extracellular matrix (ECM). Studies of cellular communication and signaling have historically focused on chemical pathways. However, the role of physical cues exchanged among cells and through the ECM is increasingly being recognized as an important mediator of cellular sensing and communication. For example, the stiffness of the ECM has profound impacts on cell morphology and cytoskeletal structure (1) and on stem cell differentiation (2, 3) and is associated with tumor formation (4, 5). Sensitivity to physical cues within the microenvironment demonstrates that cells are able to convert mechanical signals into biochemical signals. Conversely, cells remodel their surrounding ECM in response to specific chemical cues. For example, secretion of transforming growth factor β (TGF- β) or the absence of tumor necrosis factor α (TNF- α) leads to increased fibrosis and increased stiffness of the ECM (6, 7). Therefore, cells transduce chemical signals into physical signals that trigger changes in nearby cells. Mechanotransduction is a dynamic process that plays a critical role in the survival of multicellular organisms.

It has long been known that stretching of nerve cells leads to cellular depolarization (8). The mechanism, however, by which this mechanical stimulation is transduced into a chemical signal was not confirmed until Guharay and Sachs (9) later reported the presence of mechanosensing ion channels in muscle cells. These ion channels are a critical feature of specialized force-sensing cells, such as hair cells in the inner ear (10). In the 30 years since this discovery, many additional mechanotransduction pathways have been identified. Typically, the mechanisms employed involve force-induced conformational changes in a protein that trigger additional protein-protein interactions. For example, the mechanical unfolding of fibronectin, an ECM protein, has been shown to expose cryptic binding sites that allow fibronectin cross-linking (11, 12), thus providing a method for cells to mechanically manipulate and remodel the structure of their surrounding ECM. An additional example is talin, an adaptor protein in focal adhesions (FAs), which has been reported to reveal additional sites for

vinculin binding in response to mechanical strain (13). The increase in vinculin binding under strain results in reinforcement of the attachment of the FA to the cytoskeleton (13, 14). Another FA adaptor protein, p130Cas, exposes tyrosine phosphorylation sites for Src family kinases when stretched, suggesting an additional force-sensitive aspect of FA signaling and regulation (15). Gaining a molecular-level understanding of these and other mechanotransduction processes is of fundamental importance to cell biology.

Early topics in the field of cellular mechanotransduction, some of which are still being actively investigated today, include the study of cellular adhesion forces, stiffness characteristics of intact cells, cellular stiffening and chemical responses to applied forces, and the viscoelastic properties of cells. Methods used to conduct these studies include atomic force microscopy (AFM) (16–20), magnetic twisting cytometry (21–25), particle tracking rheology (26–31), and laser ablation of cytoskeletal structures (32–36). Given the interdisciplinary nature of mechanotransduction studies, advances in the field have been heavily dependent on technique development. Specifically, methods to measure and apply forces have been central to defining the types of biological questions that could be pursued.

Due to tremendous advances in single-molecule techniques, there has been a recent trend of investigating mechanotransduction events on a molecular scale. In fact, a vast number of quantitative molecular tension measurements have been obtained from single-molecule techniques, such as AFM (19, 37–43) and tech-

Accepted manuscript posted online 1 June 2015

Citation Jurchenko C, Salaita KS, 2015. Lighting up the force: investigating mechanisms of mechanotransduction using fluorescent tension probes. *Mol Cell Biol* 35:2570–2582. doi:10.1128/MCB.00195-15.

Address correspondence to Khalid S. Salaita, ksalaita@emory.edu.

Copyright © 2015, American Society for Microbiology. All Rights Reserved. doi:10.1128/MCB.00195-15

niques involving optical and magnetic tweezers (13, 14, 44–51) and biomembrane force probes (52–55). Primarily, these measurements are performed *in vitro* and typically require that the experimenter apply a force to a protein complex. When researchers are able to perform these experiments with live cells, they interrogate receptors on the membrane but not cytosolic proteins. Thus, there remain questions about how or whether many mechanotransduction events occur *in vivo* and whether force-induced changes are used by the cell to regulate function. Live-cell experiments, which measure tension within the cell or applied by the cell, have the potential to inform our understanding of chemomechanical coupling and are particularly relevant for trying to understand the formation of protein assemblies and how force is propagated through these assemblies to initiate biochemical responses in the cell.

Currently, the field of mechanotransduction is undergoing rapid growth due, in part, to the availability of new fluorescence-based molecular tension-sensing probes that report forces for discrete, site-specifically labeled molecules. These sensors are filling the need for molecularly specific, quantitative force imaging methods. The advent of these probes is allowing the research community to explore molecular tension events and to correlate these events with biochemical processes in live cells. This minireview gives a brief overview of the history of measuring cellular forces and summarizes the state of the art in performing such measurements and how it is transforming the field of mechanotransduction.

FOCAL ADHESIONS AS A MODEL MECHANOTRANSDUCTION SYSTEM

Physical sensing of the microenvironment and remodeling of the ECM are mediated by protein assemblies that form at the cell-ECM junction. The primary proteins linking the cell to the ECM are the integrin receptors, which are responsible for directly binding and bridging the intracellular cytoskeleton with the ECM (56). Once ligand bound, the integrin receptors typically cluster, recruit intracellular adaptor and signaling proteins, and form FAs. Given that integrins experience a significant mechanical load and also display differential ligand affinities as a function of matrix stiffness, integrin-based FAs have quickly become the prototypical model for studying mechanotransduction.

Many methods have been applied to study the potential role of force in integrin-ECM binding and subsequent FA formation. For example, Jiang et al. (57), using a laser-trapped bead, observed a 2-pN slip bond between the ECM protein fibronectin (Fn) and the integrin $\alpha_5\beta_3$ /talin 1/F actin complex. In this work, the 2-pN bond was hypothesized to represent the force at which the connection to the cytoskeleton is disrupted. Additional work by Roca-Cusachs et al. (58) used magnetic tweezers to explore how Fn clustering modulates cell adhesion strength. They found that cells bound to Fn pentamers could withstand ~6-fold-greater forces before rupture of the bond than Fn monomers. Furthermore, $\alpha_5\beta_1$ integrins were primarily responsible for maintaining adhesion strength, while $\alpha_5\beta_3$ integrins responded to mechanical stimulation by inducing cellular stiffening, likely through recruitment of more integrins, adaptor proteins, or cytoskeletal attachments to reinforce adhesion sites. They also noted that integrin clustering is required for binding of talin to cytoplasmic integrin tails.

Additional methods for observing and analyzing cellular traction forces include traction force microscopy (TFM) (59–63) and

micropillar array detectors (mPADs) (64–72). TFM and mPADs are designed to detect cellular forces applied to the ECM by observing deformation of the underlying substrate. In the standard TFM experiment, cells are cultured on hydrogels containing fluorescently labeled beads, and cell traction force measurements are based on measuring bead displacement while accounting for the elasticity (or resistance) of the substrate. When mPADs are used, the gel is patterned into micrometer-sized polydimethylsiloxane (PDMS) posts onto which cells are cultured. Deformation, or bending, of the posts is measured optically to infer lateral forces. These methods have greatly contributed to the field of mechanotransduction. High-resolution TFM experiments have revealed that FAs contain both stable, static states and dynamic, sampling states that allow the cell to sense its physical environment (73). TFM studies, coupled with small interfering RNA (siRNA) knock-down, by Prager-Khoutorsky et al. (74) identified several protein tyrosine kinases that appear to play a role in force application through FAs. However, estimating single-molecule forces using these methods requires assessing the local density of receptors and averaging of substrate stress across micrometer-sized regions. Therefore, while these methods are valuable, they are not well suited to the study of molecular-scale forces.

Determining polymer deformation using fluorescence resonance energy transfer (FRET), rather than bead or pillar displacement is, in principle, capable of tracking nanometer scale deformations, thus potentially offering greater sensitivity. FRET is a mechanism of nonradiative energy transfer from one fluorophore (donor) to another fluorophore (acceptor). The efficiency of energy transfer is dependent on the donor-acceptor distance and the alignment of the fluorophore transition dipole moments (75). Pairs of fluorophores, which have spectral overlap between the donor emission and the acceptor absorbance, have a characteristic distance (Förster distance, or R_0) at which energy transfer efficiency is equal to 50%. R_0 values are typically in the range of 4 to 7 nm. Due to nanometer sensitivity, FRET is routinely used to quantify conformational dynamics in single molecules (76–80) and has been used in several biosensors designed to detect activated forms of specific proteins, such as Src kinase (81–84), focal adhesion kinase (FAK) (85), and the GTPases Rac (84, 86) and RhoA (87, 88). These types of biosensors were the original inspiration for many of the newly emerging molecular tension-sensing methods that are discussed in the following section. Initial approaches using FRET to determine Fn network deformation used random dye labeling of Fn. Therefore, the signal-force response function of the labeled Fn could not be calibrated to report specific forces. Thus, while these measurements were highly sensitive and could be obtained in real time, the methods generated qualitative tension maps rather than quantitative and calibrated images. For example, Baneyx et al. (89) and Smith et al. (90) labeled Fn by reacting the free cysteine residues of FnIII₇ and FnIII₁₅ with acceptor fluorophore followed by labeling of free amines with the donor dye (89). Alternatively, labeling could be achieved by coupling a 1:1 ratio of donor and acceptor fluorophore in a one-pot reaction (90). In this way, FRET was used to report on the deformation and extension of Fn fibers. As a proof of concept, fibroblasts were cultured with the Fn conjugates, and cell-driven changes in FRET were monitored. Importantly, FRET-based detection of Fn deformation was also applied to fibroblasts cultured in three-dimensional (3D) matrices (91), which more accurately represent the native cellular environment than 2D substrates. An

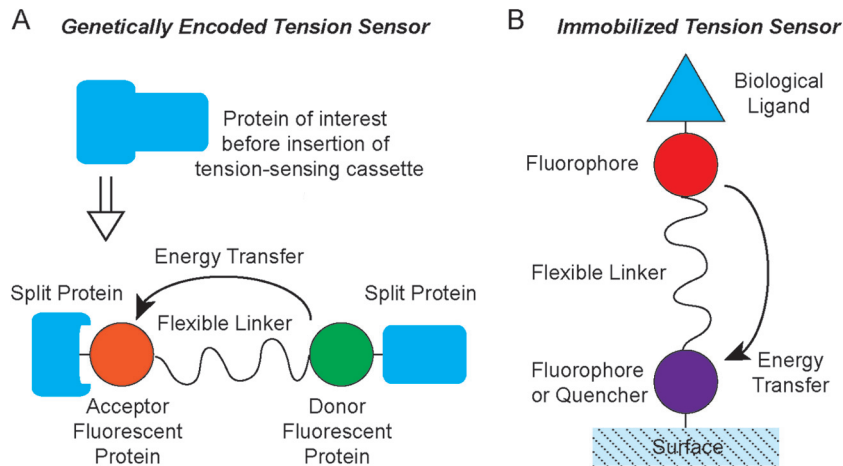


FIG 1 General schematic of genetically encoded molecular tension sensors (A) and immobilized molecular tension sensors (B). Genetically encoded tension sensors require modification of a protein to introduce a fluorescent tension-sensing module. Immobilized tension sensors are directly grafted onto cell culture substrates. Both designs employ fluorescence energy transfer to report on forces that extend a flexible linker.

alternative FRET-based method involves fluorescent labeling of a population of adhesion ligands with donor or acceptor molecules and embedding these in hydrogels. Cells cultured on the surface caused the distance between donor and acceptor chromophores to change, thus providing a FRET readout that correlated to cell-applied tension (92). While useful in providing relative FRET values, one challenge of these methods pertains to the cross-linked nature of the matrix. This results in forces being distributed across the polymer network, thus limiting the ability to quantify precise forces associated with individual adhesion receptors during cell signaling events.

Although many studies of FA mechanotransduction have been reported, there are still many questions remaining about the cellular mechanisms of mechanosensing in adhesions. For example, how does clustering of integrin receptors affect the ability of cells to apply tension? What is the loading rate of force applied by the cell and how does this affect tension? What is the amount of tension applied across an individual integrin-ECM bond? An additional question concerns the nature of the integrin-ECM bond itself. Certain integrins ($\alpha_5\beta_1$) have been shown to exhibit catch-bond behavior, in which a reduction in the receptor-ligand dissociation rate is observed in response to moderate levels of force applied across the bond (93, 94). Catch-bond behavior is in contrast to the vast majority of bonds (slip bonds), which accelerate the rate of dissociation upon application of a mechanical load (95, 96). It is not clear, however, if other integrin receptors also display a catch-bond character. Examples of proteins exhibiting catch-bond behavior include P-selectin and its ligand (97) and the $\alpha_5\beta_1$ integrin receptors bound to fibronectin (94). Recently, the E-cadherin/ β -catenin/ α E-catenin complex has also been shown to have more stable binding to F actin when ~ 5 to 10 pN of tension is applied to the bond (51). The majority of studied catch bonds are observed in the range of ~ 5 to 20 pN per receptor-ligand pair. Given the limitations of TFM, it is not possible to address these questions at this time. The inherent elasticity of TFM substrates or micropillar array substrates dictates the sensitivity of these approaches to quantify cell traction forces. However, this introduces some challenges, because the substrate elasticity also influences cell biology and cell adhesion. Thus, the measurement itself can be

confounding. Another limitation of TFM and mPADS is related to the spatial resolution, which is typically on the order of a few micrometers to $\sim 0.7 \mu\text{m}$ (63, 73). This is dictated by the density of the fiducial markers in TFM or the density and size of PDMS pillars used in mPADS (66). Finally, TFM and mPADS are sensitive to forces in the nanonewton range, which are significantly greater than the forces experienced by nascent adhesions and certainly greater than the forces experienced by individual molecules. These limitations have motivated the development of molecular tension probes, which are described in the following section.

EMERGING METHODS FOR MEASURING MOLECULAR TENSION

Recently, new methods have been developed that address the need for measuring live-cell molecular-scale forces. These molecular tension sensors contain two basic components. The first component is a pair of chromophores that act as a spectroscopic ruler through an energy transfer mechanism, such as FRET. The second component is a flexible linker that connects the two chromophores. For the purpose of this review, we have divided the molecular tension sensors into two categories, those that are genetically engineered and expressed within living cells (Fig. 1A) and those that are anchored to a surface (Fig. 1B), to probe receptor forces at the interface between living cells and their external ligands. In the case of genetically encoded tension sensors (GETS), the fluorophore and linker are inserted into a protein of interest inside the cell. In contrast, immobilized tension sensors are anchored to a substrate and present a ligand specific to a cell surface receptor (Fig. 1). The choice of fluorescent donor and acceptor, as well as the choice of linker, impacts the dynamic range and the sensitivity of the sensor by dictating the magnitude of linker extension that can be measured (thus the range of detectable forces) and the amount of fluorescent signal in the absence of force.

Most molecular tension probes utilize FRET, which requires spectrally matched fluorophores or fluorophore-quencher pairs. Fluorophores may be organic dyes or fluorescent proteins. Due to the distance dependence of FRET, placement of a flexible linker between the donor and acceptor allows fluorescence imaging to be used to detect nanometer changes in extension of the linker under

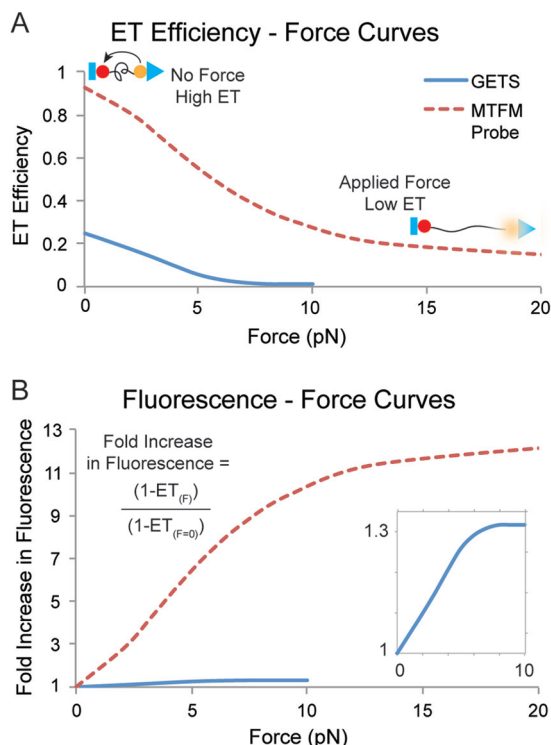


FIG 2 Plots of fluorescence as a function of force for typical genetically encoded tension sensors (GETS) and immobilized MTFM probes. (A) Plot of energy transfer (ET) efficiency as a function of applied force in units of pN. ET efficiency is dependent on the distance between donor and acceptor to the sixth power. (B) Plot of the fold increase in fluorescence as a function of force (in piconewtons). The fold increase in signal is normalized to the fluorescence signal when force is 0 pN. Fold increase in fluorescence is defined as $(1 - ET_F)/(1 - ET_{F=0})$, where ET_F is the energy transfer efficiency as a function of force and $ET_{F=0}$ is the energy transfer efficiency in the absence of force. Data for the GETS signal were estimated from the work of Grashoff et al. (98), while the data for the MTFM probes were obtained from the work of Jurchenko et al. (99).

tension. The Förster distance (R_0) of each FRET pair is critical to determining the range of distances at which the fluorophores can participate in energy transfer and therefore often limits the range of extensions and forces that can be explored.

The relationship between force and fluorescence can be assessed through experimental calibration or by using well-established models of linker behavior under force. Once a tension sensor has been shown to have a predictable fluorescence-force curve (Fig. 2), quantitative force measurements can be obtained in live cells. It is important to note that the molecular tension sensors start with some degree of donor-acceptor separation even in the absence of force, which leads to energy transfer (ET) efficiencies that are less than 100% at a force of 0 pN. The amount of fluorescent signal in the absence of force is a critical parameter, since it influences the dynamic range and sensitivity of the probe. For example, if a tension sensor has an ET efficiency of 50% in the absence of force, then the maximum increase in donor fluorescence is 2-fold over the resting value of donor emission. In contrast, a probe with 95% ET efficiency at rest can display a maximum increase in donor signal of 20-fold, which is much more desirable when live cells that exhibit autofluorescence are being imaged. Given the intrinsic dimensions of fluorescent proteins,

the typical ET efficiencies at rest for GETS are lower than that of probes employing organic dyes. To illustrate this point, Fig. 2A shows a plot of the ET efficiency as force is applied to either a GETS (blue line) (98) or an immobilized molecular tension fluorescence microscopy (MTFM) probe (red line) (99). A low ET efficiency at zero force indicates a resting conformation in which the donor and acceptor are significantly separated. The effect of low ET at the resting state is shown in Fig. 2B, where the maximum donor fluorescent signal for the GETS is ~ 1.3 -fold over the starting fluorescence intensity. The representative immobilized probe, which utilizes organic dye donor-acceptor pairs rather than fluorescent proteins, has a resting ET efficiency of ~ 0.9 . Therefore, the immobilized probe exhibits a maximum signal approximately 10-fold greater than the fluorescence intensity at zero force. Also note that, due to the nonlinear character of the fluorescence-force curves, the sensors become less sensitive to changes in force at ~ 12 pN for the representative immobilized probe and ~ 6 pN for the representative GETS.

The choice of linker between the two chromophores also plays an important role in defining the dynamic range of the sensor by tuning the “spring constant” of the probe. Each type of linker has a unique force-extension response function, and this should be well matched to the linear range of ET distances for the donor-acceptor pair. The linker may behave as an entropic spring, as is the case for polyethylene glycol (PEG) polymers, or it may contain some degree of secondary structure, such as with some peptides or proteins. An additional example linker is a DNA hairpin. This type of linker behaves more like a digital switch, abruptly denaturing and changing extension in response to a threshold magnitude of force. A summary of reported molecular tension sensors is given in Table 1.

Genetically encoded tension sensors. Genetically encoded molecular tension sensors (GETS) are engineered proteins in which a tension sensing module, or cassette, has been genetically inserted into a protein of interest. This class of probes contains two fluorescent proteins (a donor and an acceptor) and a flexible protein-based linker connecting the fluorophores (Fig. 1A). As with all of the molecular tension sensors, when the tension-sensing cassettes are being designed, concerns such as matching the R_0 of the donor-acceptor pair with the extension range of the linker must be taken into account. Then, a library (or multiple libraries with different cassette design variants) of protein mutants is created and tested to assess the best location within the protein to insert the cassette. The ideal location would be a region of the protein that maintains a relatively high ET efficiency in the absence of force and experiences forces that extend the linker during cell activity. After the site of module insertion is chosen, DNA that encodes the cellular expression of the engineered protein must be transfected into living cells, and appropriate protein expression, localization, and function must be verified. This is necessary to ensure that insertion of the ~ 60 -kDa tension sensing module does not affect, or inhibit, protein function. Several reviews have recently been published that further describe a thorough list of the control experiments and constructs that are recommended to verify that the GETS is functioning properly and not interfering with cell or protein function (100–102). Once a mutant is identified that preserves biological function and contains an appropriately placed sensor, tension across the protein can be observed in living cells using fluorescence imaging. These sensors, therefore, take time to design and engineer, but they are very simple to adopt and

TABLE 1 Comparison of molecular-force sensors^a

Type and sensor	Spectroscopic ruler	Linker	Max S/B ^b	Force dynamic range (pN)	Protein(s) targeted	Reference(s)
GETS						
stFRET	FRET	α-Helical peptide	1.8-fold	~5–7 ^c	Spectrin, α-actinin, filamin A, collagen-19	103, 104
sstFRET	FRET	Spectrin repeat	2-fold	~5–7 ^c	α-Actinin	105–107
cpstFRET	FRET	Poly(G) peptide	4-fold	~5–10 ^c	Spectrin	108
PriSSM	PRIM	AS(GGS) ₉	2-fold	ND	Myosin II	109, 111
TSMoD	FRET	(GPGGA) ₈	1.3-fold	~1–6 ^c	Vinculin, E-cadherin, VE-cadherin, PECAM, β-spectrin, MUC1	35, 98, 112–116
Immobilized						
MTFM-FRET	FRET	PEG ₂₄	10-fold	~1–20 ^d	EGFR, integrins	99, 117
MTFM-NSET	NSET	PEG ₈₀	10-fold	~1–25 ^d	Integrins	126, 127
MTFM-DNA	FRET	DNA hairpin	30-fold	~5–16 ^c	Integrins	129
TP	FRET	DNA hairpin	~30-fold	~6–17 ^c	Integrins	130
MTS	FRET	(GPGGA) ₈	3-fold	~1–7 ^d	Integrins	118, 135
TGT	NA	DNA	NA	~12–56 ^d	Integrins, Notch/Delta	131

^a ND, not determined; NA, not applicable.

^b Maximum signal/background ratio (S/B) is defined as $(1 - ET_{F_{max}})/(1 - ET_{F=0})$, where $ET_{F_{max}}$ is the energy transfer efficiency at full linker extension and $ET_{F=0}$ is the energy transfer efficiency in the absence of force.

^c The sensor response was experimentally calibrated.

^d Sensor response was determined through calculation.

use. The FRET measurement requires appropriate bleed-through and cross talk corrections, but image acquisition is relatively straightforward. Another benefit of these biologically encoded sensors is that the fluorophores are more likely to be present at a 1:1 ratio, which improves the accuracy of the FRET measurement. Since these sensors are genetically encoded, the use of fluorophores and linkers is limited to protein-based constructs. The R_0 of most fluorescent proteins is between 4 and 6 nm; therefore, the effective spring constant of the linker becomes the primary element available to the researcher to control the dynamic range of the sensor. This makes the choice of linker critical to the effectiveness of the sensor and requires that the dynamic range match the range of forces that are expected in the system under investigation.

In 2008, Meng and coworkers reported one of the first biologically engineered tension sensors (103). This sensor, which was termed a stretch-sensitive FRET cassette (stFRET), consisted of two fluorescent proteins, Cerulean and Venus, joined by a 5-nm protein α-helix (Fig. 3A). As a proof of concept, the stFRET was inserted into several different proteins (spectrin, α-actinin, and filamin A) and expressed in cultured cells (103). Insertion of the stFRET into α-actinin revealed a decrease in tension at the lagging edge of 3T3 fibroblasts (Fig. 3B). Furthermore, by inserting the sensor into collagen, Meng et al. were able to express it in a living host, *Caenorhabditis elegans* (103, 104). The initial work, however, did not include a calibration of the sensor; thus, no quantification of the observed forces was possible. In later work, the sensitivity range of the stFRET was determined to be 5 to 7 pN by using DNA hybridization to generate a force and extend the sensor (104, 105). FRET measurements of the stFRET probe indicate that the probe is slightly extended when conjugated to single-strand DNA (ss-DNA) (prior to DNA hybridization). This suggests that the force dynamic range of the stFRET is slightly larger than the 5- to 7-pN range and that the probe is more likely analog than digital. However, unambiguous calibration of this probe needs to be performed using a single-force spectroscopy experiment in order to determine its response function. The sensor was also improved

(and renamed the spectrin repeat stretch-sensitive FRET sensor [sstFRET]) by substituting a spectrin repeat for the α-helix initially used as the linker (105). This updated sensor was then used to observe mechanical behavior in α-actinin under shear stress (106) and during FA growth (107). A further modification of the sensor utilized circular permutants of Cerulean and Venus to create a probe (termed cpstFRET) in which the fluorophores are closely linked and the tension signal is due to changes in the angle between the two proteins (108).

Another genetically engineered strain sensor was reported by Iwai and Uyeda (109). This sensor, named the proximity imaging (PRIM)-based strain sensor module (PriSSM), is based on proximity imaging of green fluorescent protein (GFP) (Fig. 3C). PRIM compares the ratio of emission at 510 nm when GFP is excited at 395 and 475 nm (110). When two GFPs dimerize, this ratio shifts, and thus, the change in proximity can be monitored. In order to generate an effective sensor, Iwai and Uyeda made a GFP circular permutant, which created new termini in one of the GFP monomers. This allowed the linker to connect the two monomers with minimal steric inhibition caused by their natural antiparallel dimerization. The linker chosen for PriSSM was a flexible 29-amino-acid peptide linker. By incorporating the PriSSM into myosin II, researchers were able to observe myosin interaction with F actin (Fig. 3D) (109, 111). These experiments allowed the localization of myosin directly interacting with F actin to be determined in live cells.

In 2010, Grashoff et al. designed a tension sensor module (TSMoD) which contained mTFP1 and Venus (A206K) as the fluorescent proteins and used a 40-amino-acid sequence derived from spider silk protein as the flexible linker (Fig. 3E) (98). The dynamic range of the TSMoD was calibrated using single-molecule fluorescence imaging coupled with optical tweezers, which represented an important step in the field. In order to facilitate the single-molecule measurement, the ends of the linker were labeled with the organic dyes Cy3 and Cy5, and by using optical tweezers, this construct was stretched and the resulting fluorescence

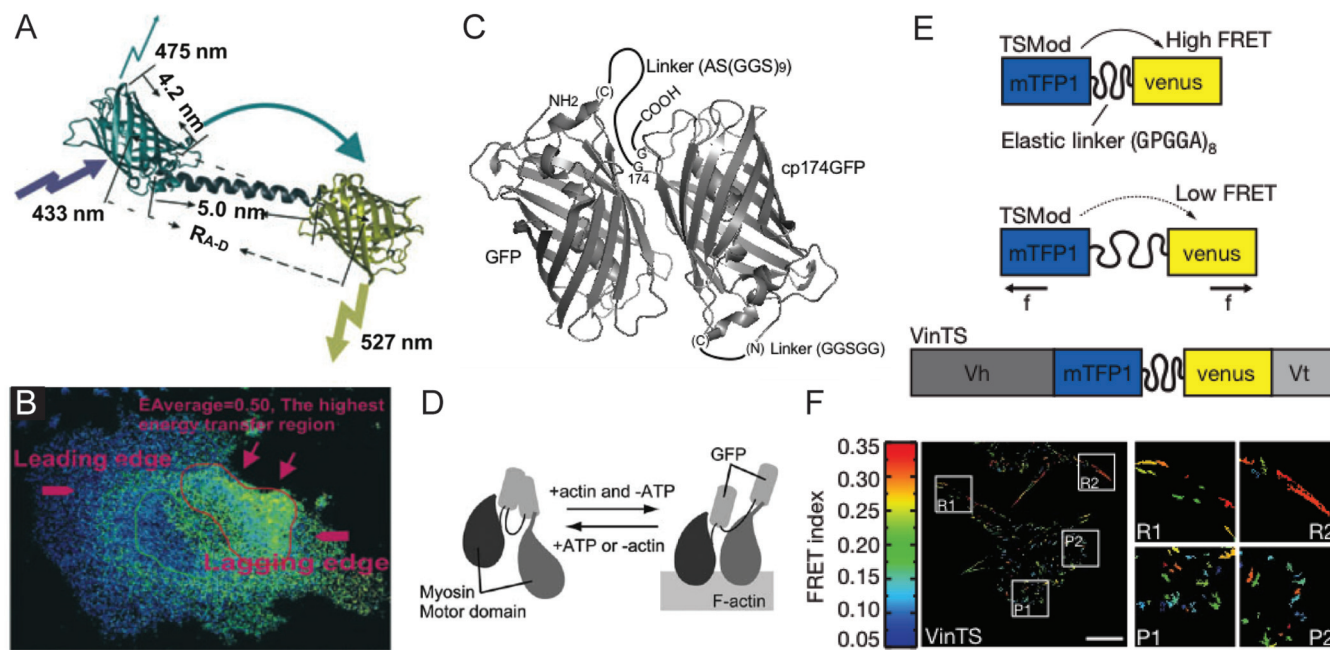


FIG 3 Examples of genetically engineered molecular tension sensors. (A) FRET cassette (stFRET) designed by Meng et al. (103). (B) Data from 3T3 cells containing the stFRET showing decreased tension in α -actinin at the lagging edge of the cell. (Images in panels A and B are reprinted from reference 103 with permission of the publisher.) (C) A PRIM-based strain sensor module (PriSSM) reported by Iwai and Uyeda (109). (D) Schematic of the incorporation of PriSSM into myosin. (Images in panels C and D are reprinted from reference 109 with permission of the publisher.) (E) Tension sensor module (TSMOD) designed for insertion into vinculin by Grashoff et al. (98). (F) Cells containing the TSMOD inserted into vinculin reveal higher tension (low FRET index) in regions of cell protrusion (P1 and P2) compared to regions where the cell retracts (R1 and R2). (Images in panels E and F are reprinted from reference 98 with permission of the publisher.)

changes recorded. TSMOD was then incorporated into vinculin to observe tension during cell migration, revealing an increase in tension across vinculin within FAs at the protruding edges of the cell (Fig. 3F). Vinculin was reported to experience an average force of 2.5 pN.

Currently, the TSMOD probe is widely being adapted by many different research groups to test forces in a range of proteins and cellular signaling pathways. For example, it is now being used to explore the role of mechanical force across proteins in cellular systems that include E-cadherin (112, 113), VE-cadherin, and PECAM (114). Additionally, incorporation of the TSMOD into β -spectrin in *C. elegans* allowed researchers to explore the role of β -spectrin in touch receptors in living organisms (115). It has also been used in conjunction with another method to study cellular traction forces, laser ablation of cytoskeletal stress fibers (35), and was recently employed as a compression sensor to study the effect of the glycocalyx on integrin activation and FA formation in cancer cells (116).

Although the use of TSMOD in cell mechanotransduction studies is expanding, certain limitations should be noted. The low sensitivity of the GETS presents some challenges. For example, when data from fluorescence images are analyzed, it is critical to differentiate between applied tension and other factors that may also contribute to a low ET efficiency, such as low sensor incorporation or high autofluorescence from the cell. To ensure that the observed data are quantitative, a method such as fluorescence lifetime imaging microscopy (FLIM) or normalization of fluorescence to either the donor or acceptor fluorophore emission needs to be applied. Furthermore, even under ideal imaging conditions, the GETS that have thus

far been reported are limited to the detection of forces within the range of 1 to 7 pN (98, 104). Another limitation pertains to the potential non-wild-type activity of engineered proteins in which the tension sensing module is embedded. Finally, GETS probes are difficult to integrate with other FRET based biosensors due to spectral overlaps.

Immobilized tension sensors. Immobilization of molecular tension sensors to a solid support allows forces between cell membrane receptors and their extracellular ligands to be investigated. These interface sensors are ideally suited to study molecular interactions that contribute to cell-cell or cell-ECM adhesion. Anchored tension probes reveal details about how cells relay mechanical signals from their surroundings into intracellular chemical cascades.

The first immobilized molecular tension sensor specific to cell surface receptors was reported by our group in 2012 and revealed the force exerted during endocytosis of the epidermal growth factor receptor (EGFR) after ligand binding (Fig. 4A) (117). This tension-sensing method was termed molecular tension fluorescence microscopy (MTFM) (99). The original MTFM sensor consisted of a synthetic fluorophore-quencher pair connected by a PEG linker anchored to the surface of a glass slide through streptavidin-biotin binding. Using a nonradiative chromophore as the FRET acceptor allows the sensor output to be a read as a simple “turn on” signal without the need to perform corrections for spectral bleed-through or cross talk. Additionally, since only one fluorescence channel is needed for force imaging, it leaves 2 or 3 channels available for the imaging of downstream cellular signaling in response to tension. For example, FRET biosensors such as FAK (85) and Src

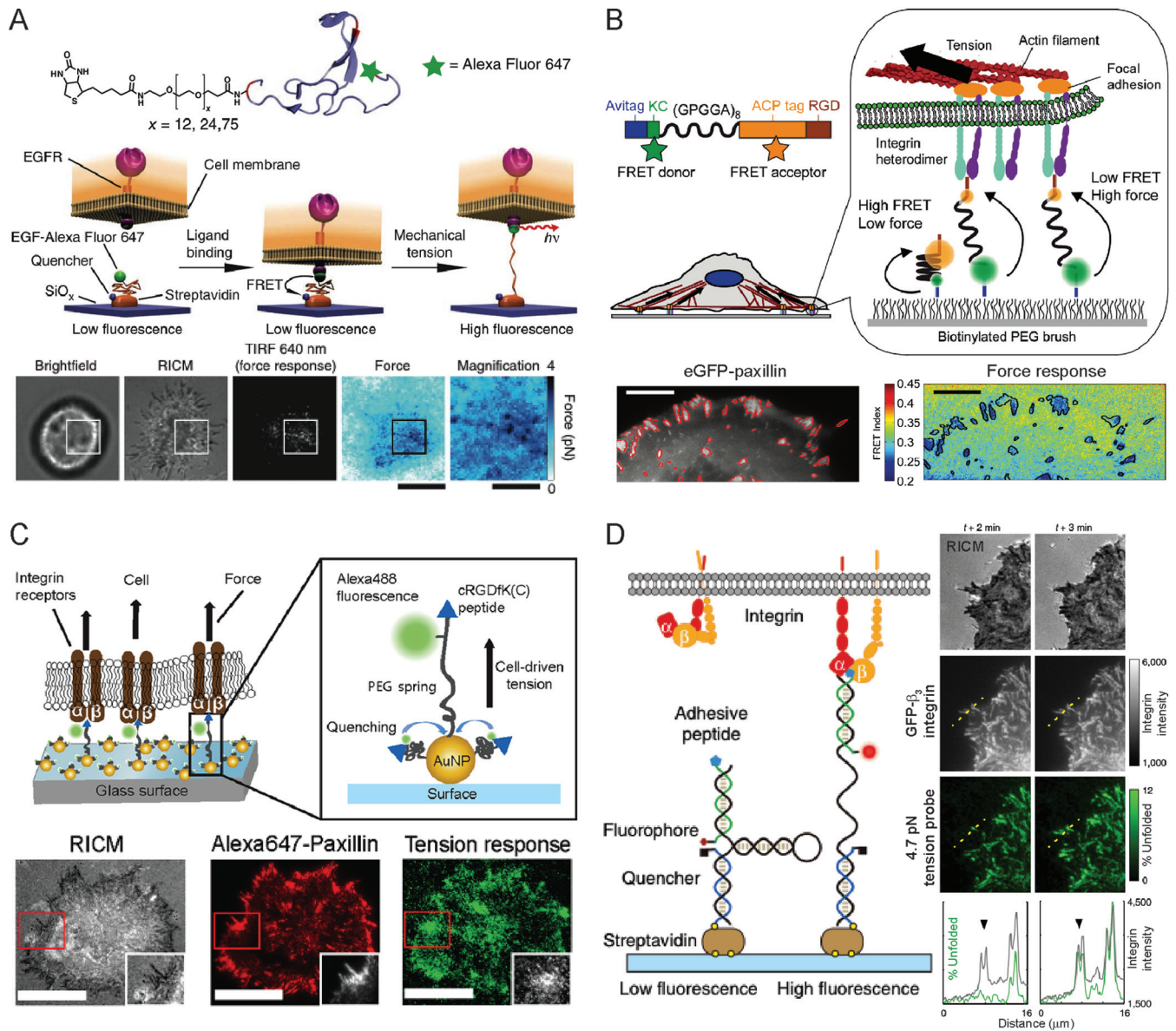


FIG 4 Examples of immobilized molecular tension sensors. (A) Schematic and representative data for a MTFM probe designed to detect forces associated with endocytosis of the EGF ligand by its receptor. (Reprinted from reference 117 with permission of the publisher.) (B) Immobilized tension sensor that was modeled on the genetically encoded TSMOD. The spider silk protein domain (GPGGA)₈ was used as the linker, and Alexa Fluor 546 and 647 were used as the donor and acceptor. (Left) Location of FAs (circled in red), as indicated by fluorescent labeling of paxillin. (Right) Regions of tension (lower FRET index) that colocalize with FAs. (Reprinted from reference 118 with permission of the publisher.) (C) AuNP-based MTFM sensor that utilizes NSET as a spectroscopic ruler. This probe primarily reported the tension observed between $\alpha_v\beta_3$ integrins and cRGD. (Reprinted from reference 126 with permission of the publisher.) (D) Schematic and representative data of DNA-based MTFM probes that display a digital output. When sufficient force is applied (4.7 pN), the DNA hairpin is unfolded, leading to separation of the fluorophore from the quencher and an increase in fluorescence of ~20- to 30-fold. Cells expressing β_3 -integrin-GFP were cultured on the DNA-MTFM probes. Images on the right show two different time points, correlating to the arrival of β_3 integrins (black line scan) followed by the appearance of tension (green line scan). (Reprinted from reference 129 with permission of the publisher.)

biosensors (81, 82) and ratiometric Ca^{2+} indicators can be combined with MTFM probes. The dynamic range of the MTFM sensor can be calculated by applying the extended worm-like chain model to the extension of the PEG polymer. This model allows the fluorescence signal and FRET efficiency to be converted into an estimated per-ligand force value. These values, however, represent the minimum average force applied per receptor. This is due to the ensemble nature of the FRET measurements and is true for all of the molecular tension sensors, including those that are genetically incorporated. By using

extremely low densities of immobilized sensors (as was shown by Morimatsu et al. [118]), single-molecule FRET measurements can provide the absolute extension of single molecules, which eliminates the ensemble nature of the measurements. However, single-molecule measurements introduce other challenges due to the need for O_2 scavengers and the scarcity of reporters.

The MTFM tension probe was also adapted for studying FA maturation by targeting integrin receptors via a cyclic RGD (cRGD) ligand (99). However, in these experiments, it was found

that the forces applied through integrin receptors were sufficient to dissociate the streptavidin-biotin bond. Mechanical streptavidin-biotin dissociation was unexpected, because the reported K_D (affinity) for streptavidin-biotin is at least 10^6 times greater than that of the integrin-ligand bond (119–121). In addition, dissociation rates (k_{off}) predict that the integrin receptors ($k_{\text{off}} = 0.072 \text{ s}^{-1}$ at 37°C) (122) would dissociate before streptavidin-biotin dissociation ($k_{\text{off}} \sim 10^{-5} \text{ s}^{-1}$ at 37°C) (99, 123, 124). Streptavidin-biotin dissociation within a 45-min time window suggests that integrin receptors apply forces to ECM ligands that exceed 20 pN. This is because a constant force of 20 pN is required to dissociate streptavidin-biotin within the 45 min of cell adhesion (125). That said, the biological loading rate is unknown, and how it impacts the bond rupture force may be significant. In contrast to these results, researchers using an alternate design of an immobilized sensor found that integrin receptors apply 1 to 5 pN of tension to their ligand (118). These experiments utilized the spider silk protein linker developed for the TSMOD, which has a dynamic range of 1 to 6 pN. The construct was anchored to a surface via biotin-NeutrAvidin binding (Fig. 4B), and the authors (118) claimed that this bond was stable against integrin forces. The use of a linear RGD ligand in these experiments could affect the degree of force applied by the receptors, since it is known that the binding constant for integrins with certain cyclic RGD peptides is significantly greater than that for the linear RGD form (120, 121). Nonetheless, it is important to note that the attachment method of the anchored sensors must be sufficiently stable to withstand the biological forces being applied by the system.

An alternate approach to address the need for robust immobilization chemistry that is stable against mechanical dissociation yet is still compatible with MTFM probes is the use of gold-thiol (Au-SH) binding (Fig. 4C). Using Au-SH binding is extraordinarily facile and avoids the need for a small-molecule quencher, since Au films and Au nanoparticles are effective quenchers. This type of MTFM sensor, developed by Liu et al. (126, 127), anchored a cRGD ligand to a gold nanoparticle (AuNP) through a PEG linkage and was sufficiently robust to withstand integrin-mediated tension. Since the AuNP in this probe acted as both the anchor and the quencher, the energy transfer mechanism in this probe is described as nanometal surface energy transfer (NSET) mechanism. Unlike FRET-based sensors, where energy transfer efficiency is dependent on the fluorophore-quencher distance with a $1/r^6$ relationship, energy transfer efficiency in NSET has a $1/r^4$ dependence. This distance dependence results in a more linear regimen of fluorescence-distance response for NSET-based probes than is seen with FRET. In addition, NSET is highly efficient and typically displays larger R_0 values, thus probing greater distances. Lastly, NSET efficiency has a weaker dependence on fluorophore transition dipole orientation and is therefore able to provide a more robust readout than FRET (128).

An additional advantage to using AuNP-based molecular tension sensors is the ability to pattern nanoparticles and explore the impact of clustering on force dynamics. Using the AuNP MTFM sensor, Liu et al. were able to determine that $\alpha_v\beta_3$ integrins exerted less force on cRGD ligands when receptors were separated by distances of 100 nm than when they were spaced by 50 nm (127). These experiments highlight the importance of molecular assemblies in the ability of cells to apply forces to the ECM and raises further questions regarding how these assemblies contribute to cellular adhesion and sensing of the surrounding physical envi-

ronment. It also suggests that ligand spacing may be detected using mechanical sensing mechanisms.

To determine the magnitude of tension experienced by integrins during FA formation, it is necessary to avoid ensemble averaging. One solution to this problem is the use of single-molecule imaging, which was explored by Morimatsu et al. (118). Given the challenges inherent in single-molecule imaging, our lab, along with the Chen lab, developed digital tension sensors. These digital probes utilize a DNA hairpin as the linker rather than an entropic PEG spring (Fig. 4D) (129, 130). Our version of these probes employed three DNA strands, one containing a hairpin with a calibrated force threshold of unfolding and two that hybridize to the termini of the hairpin strand. These two strands act as arms to anchor the hairpin sensor to the surface and to present the cell adhesion ligand. A fluorophore and a quencher attached to the two DNA arms maintain close proximity when the hairpin is folded. When sufficient force is applied to open the hairpin the fluorophore is separated from the quencher, thus leading to an increase in signal. The version of the DNA hairpin sensor developed by Blakely et al. (130) employs a single strand of DNA. This oligonucleotide contains the hairpin, the fluorophore-quencher pair, and the anchoring molecule. These sensors were functionalized with a linear or cyclic RGD ligand and were used to investigate forces applied by integrin receptors. Experiments revealed that integrin forces were highly dynamic and heterogeneous (129, 130).

Another class of probes that use the dehybridization of DNA to investigate the magnitude of tension across integrin-ligand bonds was reported by Wang and Ha (131) and termed the tension gauge tether (TGT). The TGT consists of cRGD ligands bound to a surface by dsDNA that exhibits a known tension tolerance (T_{tot}). The T_{tot} is defined as the amount of tension required to rupture the dsDNA tether in less than 2 s under constant force. In order to examine the amount of mechanical tension required by cells to trigger adhesion and FA formation, cells were plated onto the TGT surface, and cell adhesion was monitored by phase-contrast microscopy. Surprisingly, these experiments revealed that initial cellular adhesion applies at least 33 to 43 pN of force to the substrate and that this tension, common to all cell types tested, is likely controlled by membrane tension mediated through integrin receptors. Furthermore, FA and cytoskeletal stress fiber formation required ~ 56 pN of tension applied by integrins. The TGT system was also used to examine forces involved in Notch receptor activation. However, experiments were unable to verify a specific force requirement for Notch activation.

OUTLOOK

Molecular tension sensors have improved our ability to observe and study molecular forces in real time within living cells. One of the remaining challenges for these probes is to move away from ensemble averaging of forces to determine the level of tension per protein. The ability to achieve this would allow us to answer questions such as whether integrin receptors within focal adhesions experience similar forces or a range of dynamic and transient forces and whether the force propagated through focal adhesions is disseminated equally among all integrin receptors in the complex. The most obvious method to answer these questions involves single-molecule fluorescence microscopy using molecular tension probes. However, genetically encoded sensors require the use of fluorescent proteins, which represent a challenge for single-molecule studies. Compounding this challenge is the difficulty in con-

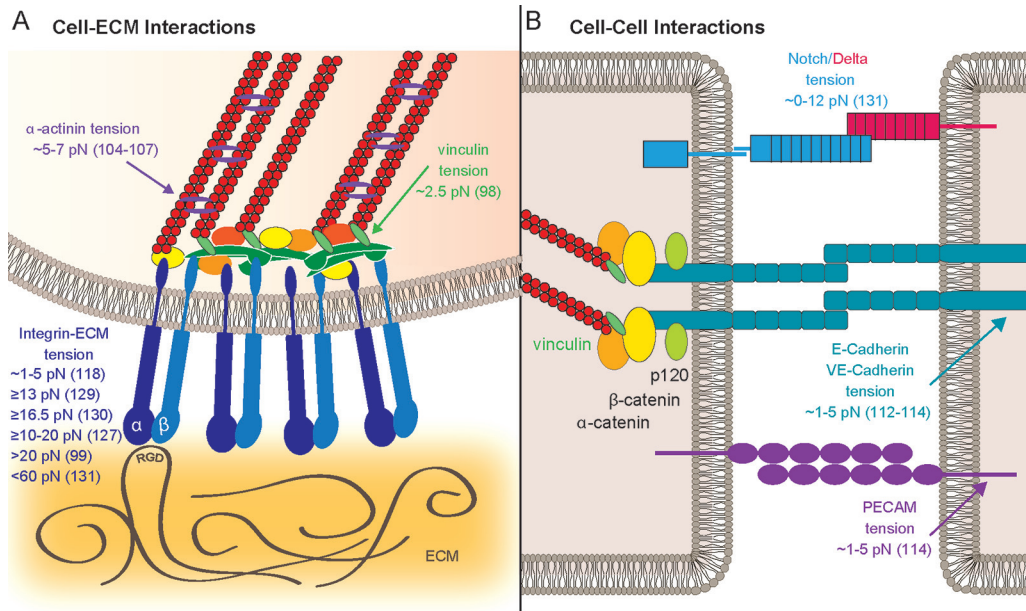


FIG 5 Schematic summary of tension values reported using molecular tension-sensing probes. (A) Cell-ECM interactions, typified by focal adhesions. Tension in α -actinin was measured using stFRET or sstFRET, while vinculin tension was determined using the TSMoD. Estimates of integrin-ECM tension were obtained using different types of immobilized molecular probes, including standard FRET-based MTFM, AuNP MTFM, DNA-hairpin sensors, and TGTs. Note that listed values were obtained using different cell types, different types of ECM ligands, and different classes of tension probes. (B) Representative schematic showing cell-cell interactions, such as cadherin complexes and Notch-Delta binding. Tension values applied by the Notch-Delta pathway, as tested by the TGT system, were reported to be either zero or less than 12 pN. E-cadherin, VE-cadherin, and PECAM tension was determined using the TSMoD inserted into the cytoplasmic sites of the protein of interest.

trolling the number and density of genetically encoded sensors expressed in the cell. Immobilized sensors show more promise in this area, but obtaining a sparse density of tension sensors to image a few of the thousands of receptors within the functional focal adhesion offers only a limited view of the entire picture, where forces are precisely orchestrated in space and time. Another approach to address this challenge may be through superresolution fluorescence microscopy techniques (132, 133). Already, the superresolution technique iPALM (interferometric photoactivatable localization microscopy) has been used to determine the localization of proteins within FAs with nanometer resolution (134). An additional superresolution imaging technique, Bayesian localization microscopy, has been used to image force in FAs using an immobilized sensor (135). It is likely that the combination of molecular tension sensors with superresolution techniques will become a rich area for exploration in mechanotransduction.

A benefit of the molecular tension sensors is the ability to observe downstream chemical signaling concurrent with fluorescence signals associated with tension. This allows one to correlate tension with specific cellular events. However, spectrum limitations can be challenging when downstream signaling is being explored. Since these sensors employ FRET as the signal output, only one fluorescence signal (or possibly two) can be used to monitor additional protein behavior in the cell in order to minimize confounding signals due to fluorescence bleed-through or cross talk. Sensors that use fluorescence quenchers rather than fluorescent FRET pairs have an advantage in this area, since more of the spectrum is available for tracking additional signals. For sensors that require two protein fluorophores, such as the genetically encoded sensors, this presents a challenge. Advanced imaging techniques,

such as spectral imaging with linear unmixing, could present a solution to imaging with multiple fluorophores (136).

There are still many questions yet to be answered regarding the role that biophysical signals play in cellular biology. As can be seen in Fig. 5, tension values have been obtained for several cell adhesion proteins using the molecular tension probes discussed in this review. However, these values are not always consistent across various techniques, and more experiments need to be performed to address this issue. Experiments with integrin receptors, specifically, have produced a wide range of estimates for tension. This may be a reflection of differences between the various tension observation techniques, including the use of different versions of ECM ligands. It may also suggest that forces applied by the cell through integrin receptors are highly dynamic. Also, differences in the force loading rate across the receptors may result in tension probe signals that vary dramatically. However, as yet, there are no robust methods to measure molecular force loading rates applied by cells. Additionally, targeting of specific integrin heterodimers with molecular tension probes has so far been limited to $\alpha_v\beta_3$. It would be interesting to see molecular tension probe studies that uniquely target other integrins, such as $\alpha_5\beta_1$, since catch-bond behavior has been reported only with $\alpha_5\beta_1$ integrins. There are also other FA-related proteins that have yet to be explored, such as the many adaptor proteins associated with FAs. The family of cadherins are beginning to be addressed, but there are still gaps in our knowledge. N-cadherin tension has not been explored, nor has vinculin been explored in the context of cell-cell junctions. PECAM has been shown to be responsive to tension, but many other cell adhesion molecules may be involved.

There are hundreds of signaling pathways with the potential of

having sensitivity to physical inputs. For example, the Notch signaling pathway, which is universally conserved across all metazoa and is fundamental to cell-cell communication and cell fate determination, has long been suspected of mechanical sensitivity. Notch receptors and their ligands are presented on the surfaces of two different cells, one that is signal sending (ligand cell) and one that is signal receiving (Notch cell). Activation of the receptor requires physical contact between the two cells. Notch contains a metalloprotease cleavage site hidden within the protein that is hypothesized to be exposed only when force is applied (137, 138). Therefore, proteolysis, leading to activation of the receptor, is suspected of being force dependent. In this case, endocytosis of the Notch-ligand complex by the ligand-expressing cell is thought to supply the force (139). Several lines of evidence have led to this hypothesis. For example, free ligand or mobile ligand does not typically activate Notch as well as bound or immobilized ligand (141, 142). Experimental evidence confirming the mechanism of force-mediated Notch activation in living cells is not yet conclusive. These studies have not been able to rule out the role of clustering in Notch activation. It has been shown that preclustered soluble ligand is capable of inducing Notch activation (143) while, in general, soluble ligand is not an efficient activator and, in some cases, can actually inhibit Notch signaling (141). Therefore, the question of how the Notch-ligand interaction leads to activation of the Notch receptor has not been fully resolved. The question of how Notch is activated represents a typical mechanistic challenge that faces the field of mechanotransduction.

Another frontier for mechanotransduction pertains to cell-pathogen interactions, which are already suspected of involving mechanics. For example, HIV-1 infection of T cells was shown to be mediated, in part, through force-mediated extension of the CD4 receptor (144). Looking forward, it is likely that fluorescence-based molecular tension probes will play a critical role in unraveling the physical aspects of cell signaling.

ACKNOWLEDGMENTS

We are grateful for support from the NIH through R01-GM097399, the Alfred P. Sloan Research Fellowship, the Camille-Dreyfus Teacher-Scholar Award, and the NSF for the IDBR (1353939) and CAREER Award (1350829).

REFERENCES

1. Yeung T, Georges PC, Flanagan LA, Marg B, Ortiz M, Funaki M, Zahir N, Ming W, Weaver V, Janmey PA. 2005. Effects of substrate stiffness on cell morphology, cytoskeletal structure, and adhesion. *Cell Motil Cytoskeleton* 60:24–34. <http://dx.doi.org/10.1002/cm.20041>.
2. Engler AJ, Sen S, Sweeney HL, Discher DE. 2006. Matrix elasticity directs stem cell lineage specification. *Cell* 126:677–689. <http://dx.doi.org/10.1016/j.cell.2006.06.044>.
3. Holle AW, Tang X, Vijayraghavan D, Vincent LG, Fuhrmann A, Choi SC, del Alamo JC, Engler AJ. 2013. *In situ* mechanotransduction via vinculin regulates stem cell differentiation. *Stem Cells* 31:2467–2477. <http://dx.doi.org/10.1002/stem.1490>.
4. Paszek MJ, Zahir N, Johnson KR, Lakins JN, Rozenberg GI, Gefen A, Reinhart-King CA, Margulies SS, Dembo M, Boettiger D, Hammer DA, Weaver VM. 2005. Tensional homeostasis and the malignant phenotype. *Cancer Cell* 8:241–254. <http://dx.doi.org/10.1016/j.ccr.2005.08.010>.
5. Shi Q, Ghosh RP, Engelke H, Rycroft CH, Cassereau L, Sethian JA, Weaver V, Lippard JT. 2014. Rapid disorganization of mechanically interacting systems of mammary acini. *Proc Natl Acad Sci U S A* 111:658–663. <http://dx.doi.org/10.1073/pnas.1311312110>.
6. Leask A, Abraham DJ. 2004. TGF- β signaling and the fibrotic response. *FASEB J* 18:816–827. <http://dx.doi.org/10.1096/fj.03-1273rev>.
7. Pickup MW, Mouw JK, Weaver VM. 2014. The extracellular matrix modulates the hallmarks of cancer. *EMBO Rep* 15:1243–1253. <http://dx.doi.org/10.15252/embr.201439246>.
8. Katz B. 1950. Depolarization of sensory terminals and the initiation of impulses in the muscle spindle. *J Physiol* 111:261–282. <http://dx.doi.org/10.1113/jphysiol.1950.sp004479>.
9. Guharay F, Sachs F. 1984. Stretch-activated single ion channel currents in tissue-cultured embryonic chick skeletal muscle. *J Physiol* 352:685–701. <http://dx.doi.org/10.1113/jphysiol.1984.sp015317>.
10. Corey DP, Hudspeth AJ. 1983. Kinetics of the receptor current in bullfrog saccular hair cells. *J Neurosci* 3:962–976.
11. Zhong C, Chrzanowska-Wodnicka M, Brown J, Shaub A, Belkin AM, Burridge K. 1998. Rho-mediated contractility exposes a cryptic site in fibronectin and induces fibronectin matrix assembly. *J Cell Biol* 141:539–551.
12. Klotzsch E, Smith ML, Kubow KE, Muntwyler S, Little WC, Beyeler F, Gourdon D, Nelson BJ, Vogel V. 2009. Fibronectin forms the most extensible biological fibers displaying switchable force-exposed cryptic binding sites. *Proc Natl Acad Sci U S A* 106:18267–18272. <http://dx.doi.org/10.1073/pnas.0907518106>.
13. del Rio A, Perez-Jimenez R, Liu R, Roca-Cusachs P, Fernandez JM, Sheetz MP. 2009. Stretching single talin rod molecules activates vinculin binding. *Science* 323:638–641. <http://dx.doi.org/10.1126/science.1162912>.
14. Yao MX, Goult BT, Chen H, Cong P, Sheetz M, Yan J. 2014. Mechanical activation of vinculin binding to talin locks talin in an unfolded conformation. *Sci Rep* 4:4610. <http://dx.doi.org/10.1038/srep04610>.
15. Sawada Y, Tamada M, Dubin-Thaler BJ, Chemiavskaya O, Sakai R, Tanaka S, Sheetz M. 2006. Force sensing by mechanical extension of the Src family kinase substrate p130Cas. *Cell* 127:1015–1026. <http://dx.doi.org/10.1016/j.cell.2006.09.044>.
16. Radmacher M, Fritz M, Cleveland JP, Walters DA, Hansma PK. 1994. Imaging adhesion forces and elasticity of lysozyme adsorbed on mica with the atomic force microscope. *Langmuir* 10:3809–3814. <http://dx.doi.org/10.1021/la00022a068>.
17. Rotsch C, Jacobsen K, Radmacher M. 1999. Dimensional and mechanical dynamics of active and stable edges in motile fibroblasts investigated by using atomic force microscopy. *Proc Natl Acad Sci U S A* 96:921–926. <http://dx.doi.org/10.1073/pnas.96.3.921>.
18. Rotsch C, Radmacher M. 2000. Drug-induced changes of cytoskeletal structure and mechanics in fibroblasts: an atomic force microscopy study. *Biophys J* 78:520–535. [http://dx.doi.org/10.1016/S0006-3495\(00\)76614-8](http://dx.doi.org/10.1016/S0006-3495(00)76614-8).
19. Lehenkari PP, Horton MA. 1999. Single integrin molecule adhesion forces in intact cells measured by atomic force spectroscopy. *Biochem Biophys Res Commun* 259:645–650. <http://dx.doi.org/10.1006/bbrc.1999.0827>.
20. Charras GT, Horton MA. 2002. Single cell mechanotransduction and its modulation analyzed by atomic force microscope indentation. *Biophys J* 82:207–2981. [http://dx.doi.org/10.1016/S0006-3495\(02\)75638-5](http://dx.doi.org/10.1016/S0006-3495(02)75638-5).
21. Wang N, Butler JP, Ingber DE. 1993. Mechanotransduction across the cell surface and through the cytoskeleton. *Science* 260:1124–1127. <http://dx.doi.org/10.1126/science.7684161>.
22. Ingber DE, Prusty D, Sun Z, Betensky H, Wang N. 1995. Cell shape, cytoskeletal mechanics, and cell cycle control in angiogenesis. *J Biomechanics* 28:1471–1484.
23. Mijailovich SM, Kojic M, Zivkovic M, Fabry B, Fredberg JJ. 2002. A finite element model of cell deformation during magnetic bead twisting. *J Appl Physiol* 93:1429–1436. <http://dx.doi.org/10.1152/jappphysiol.00255.2002>.
24. Deng L, Fairbank NJ, Fabry B, Smith PG, Maksym GN. 2004. Localized mechanical stress induces time-dependent actin cytoskeletal remodeling and stiffening in cultured airway smooth muscle cells. *Am J Physiol Cell Physiol* 287:C440–C448. <http://dx.doi.org/10.1152/ajpcell.00374.2003>.
25. Trepast X, Grabulosa M, Puig F, Maksym GN, Navajas D, Farre R. 2004. Viscoelasticity of human alveolar epithelial cells subjected to stretch. *Am J Physiol Lung Cell Mol Physiol* 287:L1025–L1034. <http://dx.doi.org/10.1152/ajplung.00077.2004>.
26. Mason TG, Ganesan K, van Zanten JH, Wirtz D, Kuo SC. 1997. Particle tracking microrheology of complex fluids. *Phys Rev Lett* 79:3282–3285. <http://dx.doi.org/10.1103/PhysRevLett.79.3282>.
27. Yamada S, Wirtz D, Kuo SC. 2000. Mechanics of living cells measured by laser tracking microrheology. *Biophys J* 78:1736–1747. [http://dx.doi.org/10.1016/S0006-3495\(00\)76725-7](http://dx.doi.org/10.1016/S0006-3495(00)76725-7).

28. Valentine MT, Kaplan PD, Thota D, Crocker JC, Gisler T, Prud'homme RK, Beck M, Weitz DA. 2001. Investigating the microenvironments of inhomogeneous soft materials with multiple particle tracking. *Phys Rev E* 64:061506.
29. Tseng Y, Kole TP, Wirtz D. 2002. Micromechanical mapping of live cells by multiple-particle-tracking microrheology. *Biophys J* 83:3162–3176. [http://dx.doi.org/10.1016/S0006-3495\(02\)75319-8](http://dx.doi.org/10.1016/S0006-3495(02)75319-8).
30. Gordon VD, Valentine MT, Gardel ML, Andor-Ardo D, Dennison S, Bogdanov AA, Weitz DA, Deisboeck TS. 2003. Measuring mechanical stress induced by an expanding multicellular tumor system: a case study. *Exp Cell Res* 289:58–66. [http://dx.doi.org/10.1016/S0014-4827\(03\)00256-8](http://dx.doi.org/10.1016/S0014-4827(03)00256-8).
31. Valentine MT, Perlman ZE, Gardel ML, Shin JH, Matsudaira P, Mitchison TJ, Weitz DA. 2004. Colloid surface chemistry critically affects multiple particle tracking measurements of biomaterials. *Biophys J* 86:4004–4014. <http://dx.doi.org/10.1529/biophysj.103.037812>.
32. Heisterkamp A, Maxwell IZ, Mazur E, Underwood JM, Nickerson JA, Kumar S, Ingber DE. 2005. Pulse energy dependence of subcellular dissection by femtosecond laser pulses. *Opt Express* 13:3690–3696. <http://dx.doi.org/10.1364/OPEX.13.003690>.
33. Kumar S, Maxwell IZ, Heisterkamp A, Polte TR, Lele TP, Salanga M, Mazur E, Ingber DE. 2006. Viscoelastic retraction of single living stress fibers and its impact on cell shape, cytoskeletal organization, and extracellular matrix mechanics. *Biophys J* 90:3762–3773. <http://dx.doi.org/10.1529/biophysj.105.071506>.
34. Colombelli J, Besser A, Kress H, Reynaud EG, Girard P, Caussinus E, Haselmann U, Small JV, Schwarz US, Stelzer EHK. 2009. Mechanosensing in actin stress fibers revealed by a close correlation between force and protein localization. *J Cell Sci* 122:1665–1679. <http://dx.doi.org/10.1242/jcs.042986>.
35. Chang C-W, Kumar S. 2013. Vinculin tension distributions of individual stress fibers within cell-matrix adhesions. *J Cell Sci* 126:3021–3030. <http://dx.doi.org/10.1242/jcs.119032>.
36. Brugués A, Anon E, Conte V, Veldhuis JH, Gupta M, Colombelli J, Muñoz JJ, Brodland GW, Ladoux B, Treppe X. 2014. Forces driving epithelial wound healing. *Nat Physiol* 10:683–690. <http://dx.doi.org/10.1038/nphys3040>.
37. Li F, Redick SD, Erickson HP, Moy VT. 2003. Force measurements of the $\alpha 5 \beta 1$ integrin-fibronectin interaction. *Biophys J* 84:1252–1262. [http://dx.doi.org/10.1016/S0006-3495\(03\)74940-6](http://dx.doi.org/10.1016/S0006-3495(03)74940-6).
38. Kokkoli E, Ochsenhirt SE, Tirrel M. 2004. Collective and single-molecule interactions of $\alpha 5 \beta 1$ integrins. *Langmuir* 20:2397–2404. <http://dx.doi.org/10.1021/la035597l>.
39. Lee S, Yang Y, Fishman D, Banaszak Holl MM, Hong S. 2013. Epithelial-mesenchymal transition enhances nanoscale actin filament dynamics of ovarian cancer cells. *J Phys Chem B* 117:9233–9240. <http://dx.doi.org/10.1021/jp4055186>.
40. Friedrichs J, Taubenberger A, Franz CM, Müller DJ. 2007. Cellular remodeling of individual collagen fibrils visualized by time-lapse AFM. *J Mol Biol* 372:594–607. <http://dx.doi.org/10.1016/j.jmb.2007.06.078>.
41. Nordin D, Donlon L, Frankel D. 2012. Characterising single fibronectin-integrin complexes. *Soft Matter* 8:6151–6160. <http://dx.doi.org/10.1039/c2sm07171a>.
42. Rakshit S, Zhang Y, Manibog K, Shafraz O, Sivasankar S. 2012. Ideal, catch, and slip bonds in cadherin adhesion. *Proc Natl Acad Sci U S A* 109:18815–18820. <http://dx.doi.org/10.1073/pnas.1208349109>.
43. Sun Z, Martinez-Lemus LA, Hill MA, Meininger GA. 2008. Extracellular matrix-specific focal adhesions in vascular smooth muscle produce mechanically active adhesion sites. *Am J Physiol Cell Physiol* 295:C268–C278. <http://dx.doi.org/10.1152/ajpcell.00516.2007>.
44. Smith SB, Finzi L, Bustamante C. 1992. Direct mechanical measurements of the elasticity of single DNA molecules by using magnetic beads. *Science* 258:1122–1126. <http://dx.doi.org/10.1126/science.1439819>.
45. Keller Mayer MSZ, Smith SB, Granitzer HL, Bustamante C. 1997. Folding-unfolding transitions in single titin molecules characterized with laser tweezers. *Science* 276:1112–1116.
46. Kuo SC, Sheetz MP. 1993. Force of single kinesin molecules measured with optical tweezers. *Science* 260:232–234.
47. Alenghat FJ, Fabry B, Tsai KY, Goldman WH, Ingber DE. 2000. Analysis of cell mechanics in giant vinculin-deficient cells using a magnetic tweezer. *Biochem Biophys Res Commun* 277:93–99.
48. Hayakawa K, Tatsumi H, Sokobe M. 2008. Actin stress fibers transmit and focus force to activate mechanosensitive channels. *J Cell Sci* 121:495–503. <http://dx.doi.org/10.1242/jcs.022053>.
49. Molloy JE, Burns JE, Kendrick-Jones J, Tregar RT, White DCS. 1995. Movement and force produced by a single myosin head. *Nature* 378:209–212. <http://dx.doi.org/10.1038/378209a0>.
50. Walter N, Selhuber C, Kessler H, Spatz JP. 2006. Cellular unbinding forces of initial adhesion processes on nanopatterned surfaces probed with magnetic tweezers. *Nano Lett* 6:398–402. <http://dx.doi.org/10.1021/nl052168u>.
51. Buckley CD, Tan J, Anderson KL, Hanein D, Volkmann N, Weis WI, Nelson WJ, Dunn AR. 2014. The minimal cadherin-catenin complex binds to actin filaments under force. *Science* 346:1254211. <http://dx.doi.org/10.1126/science.1254211>.
52. Kong F, Li Z, Parks WM, Dumbauld DW, Garcia AJ, Mould AP, Humphries MJ, Zhu C. 2013. Cyclic mechanical reinforcement of integrin-ligand interactions. *Mol Cell* 49:1060–1068. <http://dx.doi.org/10.1016/j.molcel.2013.01.015>.
53. Chen W, Lou J, Evans E, Zhu C. 2012. Observing force-regulated conformational changes and ligand dissociation from a single integrin on cells. *J Cell Biol* 199:497–512. <http://dx.doi.org/10.1083/jcb.201201091>.
54. Husson J, Chemin K, Bohineust A, Hivroz C, Henry N. 2011. Force generation upon T cell receptor engagement. *PLoS One* 6:e19680. <http://dx.doi.org/10.1371/journal.pone.0019680>.
55. Liu B, Chen W, Evavold BD, Zhu C. 2014. Accumulation of dynamic catch bonds between TCR and agonist peptide-MHC triggers T cell signaling. *Cell* 157:357–368. <http://dx.doi.org/10.1016/j.cell.2014.02.053>.
56. Hynes RO. 2002. Integrins: bidirectional, allosteric signaling machines. *Cell* 110:673–687. [http://dx.doi.org/10.1016/S0092-8674\(02\)00971-6](http://dx.doi.org/10.1016/S0092-8674(02)00971-6).
57. Jiang G, Giannone G, Critchley DR, Fukumoto E, Sheetz MP. 2003. Two-piconewton slip bond between fibronectin and the cytoskeleton depends on talin. *Nature* 424:334–337. <http://dx.doi.org/10.1038/nature01805>.
58. Roca-Cusachs P, Gauthier NC, del Rio A, Sheetz MP. 2009. Clustering of $\alpha 5 \beta 1$ integrins determines adhesion strength whereas $\alpha v \beta 3$ and talin enable mechanotransduction. *Proc Natl Acad Sci U S A* 106:16245–16250. <http://dx.doi.org/10.1073/pnas.0902818106>.
59. Pelham RJ, Wang Y-L. 1999. High resolution detection of mechanical forces exerted by locomoting fibroblasts on the substrate. *Mol Biol Cell* 10:935–945. <http://dx.doi.org/10.1091/mbc.10.4.935>.
60. Dembo M, Wang Y-L. 1999. Stresses at the cell-to-substrate interface during locomotion of fibroblasts. *Biophys J* 76:2307–2316.
61. Balaban NQ, Schwarz US, Riveline D, Goichberg P, Tzur G, Sabanay I, Mahalu D, Safran S, Bershadsky A, Addadi L, Geiger B. 2001. Force and focal adhesion assembly: a close relationship studied using elastic micropatterned substrates. *Nat Cell Biol* 3:466–472. <http://dx.doi.org/10.1038/35074532>.
62. Schwarz US, Balaban NQ, Riveline D, Bershadsky AD, Geiger B, Safran SA. 2002. Calculation of forces at focal adhesions from elastic substrate data: the effect of localized force and the need for regularization. *Biophys J* 83:1380–1394. [http://dx.doi.org/10.1016/S0006-3495\(02\)73909-X](http://dx.doi.org/10.1016/S0006-3495(02)73909-X).
63. Sabass B, Gardel ML, Waterman CM, Schwarz US. 2008. High resolution traction force microscopy based on experimental and computational advances. *Biophys J* 94:201–220. <http://dx.doi.org/10.1529/biophysj.107.113670>.
64. Tan JL, Tien J, Pirone DM, Gray DS, Bhadriraju K, Chen CS. 2003. Cells lying on a bed of microneedles: an approach to isolate mechanical force. *Proc Natl Acad Sci U S A* 100:1484–1489. <http://dx.doi.org/10.1073/pnas.0235407100>.
65. Bhadriraju K, Yang M, Ruiz SA, Pirone D, Tan J, Chen CS. 2007. Activation of ROCK by RhoA is regulated by cell adhesion, shape, and cytoskeletal tension. *Exp Cell Res* 313:3616–3623. <http://dx.doi.org/10.1016/j.yexcr.2007.07.002>.
66. Yang MT, Sniadecki NJ, Chen CS. 2007. Geometric considerations of micro- to nanoscale elastomeric post arrays to study cellular traction forces. *Adv Mater* 19:3119–3123. <http://dx.doi.org/10.1002/adma.200701956>.
67. Lemmon CA, Chen CS, Romer LH. 2009. Cell traction forces direct fibronectin matrix assembly. *Biophys J* 96:729–738. <http://dx.doi.org/10.1016/j.bpj.2008.10.009>.
68. Ruiz SA, Chen CS. 2008. Emergence of patterned stem cell differentiation within multicellular structures. *Stem Cells* 26:2921–2927. <http://dx.doi.org/10.1634/stemcells.2008-0432>.
69. Liu Z, Tan JL, Cohen DM, Yang MT, Sniadecki NJ, Ruiz SA, Nelson CM, Chen CS. 2010. Mechanical tugging force regulates the size of

- cell-cell junctions. *Proc Natl Acad Sci U S A* 107:9944–9949. <http://dx.doi.org/10.1073/pnas.0914547107>.
70. Fu J, Wang Y-K, Yang MT, Desai RA, Yu X, Liu Z, Chen CS. 2010. Mechanical regulation of cell function with geometrically modulated elastomeric substrates. *Nat Methods* 7:733–736. <http://dx.doi.org/10.1038/nmeth.1487>.
 71. Lin GL, Cohen DM, Desai RA, Breckenridge MT, Gao L, Humphries MJ, Chen CS. 2013. Activation of beta 1 but not beta 3 integrin increases cell traction forces. *FEBS Lett* 587:763–769. <http://dx.doi.org/10.1016/j.febslet.2013.01.068>.
 72. Dumbauld DW, Lee TT, Singh A, Scrimgeour J, Gersbach CA, Zamir EA, Fu J, Chen CS, Curtis JE, Craig SW, Garcia AJ. 2013. How vinculin regulates force transmission. *Proc Natl Acad Sci U S A* 110:9788–9793. <http://dx.doi.org/10.1073/pnas.1216209110>.
 73. Plotnikov SV, Pasapera AM, Sabass B, Waterman CM. 2012. Force fluctuations within focal adhesions mediate ECM-rigidity sensing to guide directed cell migration. *Cell* 151:1513–1527. <http://dx.doi.org/10.1016/j.cell.2012.11.034>.
 74. Prager-Khoutorsky M, Lichtenstein A, Krishnan R, Rajendran K, Mayo A, Kam Z, Geiger B, Bershadsky A. 2011. Fibroblast polarization is a matrix-rigidity-dependent process controlled by focal adhesion mechanosensing. *Nat Cell Biol* 13:1457–1465. <http://dx.doi.org/10.1038/ncb2370>.
 75. Lakowicz JR. 2006. Principles of fluorescence spectroscopy, 3rd ed. Springer, New York, NY.
 76. Santoso Y, Joyce CM, Potapova O, Le Reste L, Hohlbein J, Torella JP, Grindley NDF, Kapanidis AN. 2010. Conformational transitions in DNA polymerase I revealed by single-molecule FRET. *Proc Natl Acad Sci U S A* 107:715–720. <http://dx.doi.org/10.1073/pnas.0910909107>.
 77. Choi UB, Strop P, Vrljic M, Chu S, Brunger AT, Weninger KR. 2010. Single-molecule FRET-derived model of the synaptotagmin 1-SNARE fusion complex. *Nature* 17:318–325. <http://dx.doi.org/10.1038/nsmf.1763>.
 78. Ernst S, Duser MG, Zarrabi N, Dunn SD, Borsch M. 2012. Elastic deformations of the rotary double motor of single F₀F₁-ATP synthases detected in real time by Förster resonance energy transfer. *Biochim Biophys Acta* 1817:1722–1731. <http://dx.doi.org/10.1016/j.bbabi.2012.03.034>.
 79. Verhalen B, Ernst S, Borsch M, Wilkens S. 2012. Dynamic ligand-induced conformational rearrangements in P-glycoprotein as probed by fluorescence resonance energy transfer spectroscopy. *J Biol Chem* 287:1112–1127. <http://dx.doi.org/10.1074/jbc.M111.301192>.
 80. Guo Z, Noller HF. 2012. Rotation of the head of the 30S ribosomal subunit during mRNA translocation. *Proc Natl Acad Sci U S A* 109:20391–20394. <http://dx.doi.org/10.1073/pnas.1218999109>.
 81. Ting AY, Kain KH, Klemke RL, Tsien RY. 2001. Genetically encoded fluorescent reporters of protein tyrosine kinase activities in living cells. *Proc Natl Acad Sci U S A* 98:15003–15008.
 82. Wang Y, Botvinick EL, Zhao Y, Berns MW, Usami S, Tsien RY, Chien S. 2005. Visualizing the mechanical activation of Src. *Nature* 434:1040–1045. <http://dx.doi.org/10.1038/nature03469>.
 83. Na S, Collin O, Chowdhury F, Tay B, Ouyang M, Wang Y, Wang N. 2008. Rapid signal transduction in living cells is a unique feature of mechanotransduction. *Proc Natl Acad Sci U S A* 105:6626–6631. <http://dx.doi.org/10.1073/pnas.0711704105>.
 84. Ouyang M, Sun J, Chien S, Wang Y. 2008. Determination of hierarchical relationship of Src and Rac at subcellular locations with FRET biosensors. *Proc Natl Acad Sci U S A* 105:14353–14358. <http://dx.doi.org/10.1073/pnas.0807537105>.
 85. Seong J, Ouyang M, Kim T, Sun J, Wen P-C, Lu S, Zhuo Y, Llewellyn NM, Schlaepfer DD, Guan J-L, Chien S, Wang Y. 2011. Detection of focal adhesion kinase activation at membrane microdomains by fluorescence resonance energy transfer. *Nat Commun* 2:406. <http://dx.doi.org/10.1038/ncomms1414>.
 86. Kraynov VS, Chamberlain C, Bokoch GM, Schwartz MA, Slabaugh S, Hahn KM. 2000. Localized Rac activation dynamics visualized in living cells. *Science* 290:333–337. <http://dx.doi.org/10.1126/science.290.5490.333>.
 87. Pertz O, Hodgson L, Klemke RL, Hahn KM. 2006. Spatiotemporal dynamics of RhoA activity in migrating cells. *Nature* 440:1069–1072. <http://dx.doi.org/10.1038/nature04665>.
 88. Machacek M, Hodgson L, Welch C, Elliot H, Pertz O, Nalbant P, Abell A, Johnson GL, Hahn KM, Danuser G. 2009. Coordination of Rho GTPase activities during cell protrusion. *Nature* 461:99–103. <http://dx.doi.org/10.1038/nature08242>.
 89. Baneyx G, Baugh L, Vogel V. 2002. Fibronectin extension and unfolding within cell matrix fibrils controlled by cytoskeletal tension. *Proc Natl Acad Sci U S A* 99:5139–5143. <http://dx.doi.org/10.1073/pnas.072650799>.
 90. Smith ML, Gourdon D, Little WC, Kubow KE, Eguiluz RA, Luna-Morris S, Vogel V. 2007. Force-induced unfolding of fibronectin in the extracellular matrix of living cells. *PLoS Biol* 5:e268. <http://dx.doi.org/10.1371/journal.pbio.0050268>.
 91. Legant WR, Chen CS, Vogel V. 2012. Force-induced fibronectin assembly and matrix remodeling in a 3D microtissue model of tissue morphogenesis. *Integr Biol* 4:1164–1174. <http://dx.doi.org/10.1039/c2ib20059g>.
 92. Kong HJ, Polte TR, Alsborg E, Mooney DJ. 2005. FRET measurements of cell-traction forces and nano-scale clustering of adhesion ligands varied by substrate stiffness. *Proc Natl Acad Sci U S A* 102:4300–4305. <http://dx.doi.org/10.1073/pnas.0405873102>.
 93. Friedland JC, Lee MH, Boettiger D. 2009. Mechanically activated integrin switch controls $\alpha 5 \beta 1$ function. *Science* 323:642–644. <http://dx.doi.org/10.1126/science.1168441>.
 94. Kong F, Garcia AJ, Mould AP, Humphries MJ, Zhu C. 2009. Demonstration of catch bonds between an integrin and its ligand. *J Cell Biol* 185:1275–1284. <http://dx.doi.org/10.1083/jcb.200810002>.
 95. Bell GI. 1978. Models for the specific adhesion of cells to cells. *Science* 200:618–627. <http://dx.doi.org/10.1126/science.347575>.
 96. Dembo M, Torney DC, Saxman K, Hammer D. 1988. The reaction-limited kinetics of membrane-to-surface adhesion and detachment. *Proc R Soc Lond B Biol Sci* 234:55–83. <http://dx.doi.org/10.1098/rspb.1988.0038>.
 97. Marshall BT, Long M, Piper JW, Yago T, McEver RP, Zhu C. 2003. Direct observation of catch bonds involving cell-adhesion molecules. *Nature* 423:190–193. <http://dx.doi.org/10.1038/nature01605>.
 98. Grashoff C, Hoffman BD, Brenner MD, Zhou R, Parsons M, Yang MT, McLean MA, Sligar SG, Chen CS, Ha T, Schwartz MA. 2010. Measuring mechanical tension across vinculin reveals regulation of focal adhesion dynamics. *Nature* 466:263–266. <http://dx.doi.org/10.1038/nature09198>.
 99. Jurchenko C, Chang Y, Narui Y, Zhang Y, Salaita KS. 2014. Integrin-generated forces lead to streptavidin-biotin unbinding in cellular adhesions. *Biophys J* 106:1436–1446. <http://dx.doi.org/10.1016/j.bpj.2014.01.049>.
 100. Austen K, Kluger C, Freikamp A, Chrostek-Grashoff A, Grashoff C. 2013. Generation and analysis of biosensors to measure mechanical forces within cells. In Baudino TA (ed), *Cell-cell interactions*, 2nd ed. Springer, New York, NY.
 101. LaCroix AS, Rothenberg KE, Berginski ME, Urs AN, Hoffman BD. 2015. Construction, imaging, and analysis of FRET-based tension sensors in living cells. *Methods Cell Biol* 125:161–186. <http://dx.doi.org/10.1016/bs.mcb.2014.10.033>.
 102. Guo J, Sachs F, Meng F. 2014. Fluorescence-based force/tension sensors: a novel tool to visualize mechanical forces in structural proteins in live cells. *Antioxid Redox Signal* 20:986–999. <http://dx.doi.org/10.1089/ars.2013.5708>.
 103. Meng F, Suchyna TM, Sachs F. 2008. A fluorescence energy transfer-based mechanical stress sensor for specific proteins in situ. *FEBS J* 275:3072–3087. <http://dx.doi.org/10.1111/j.1742-4658.2008.06461.x>.
 104. Meng F, Suchyna TM, Lazakovitch E, Gronostajski RM, Sachs F. 2011. Real time FRET based detection of mechanical stress in cytoskeletal and extracellular matrix proteins. *Cell Mol Bioeng* 4:148–159. <http://dx.doi.org/10.1007/s12195-010-0140-0>.
 105. Meng F, Sachs F. 2011. Visualizing dynamic cytoplasmic forces with a compliance-matched FRET sensor. *J Cell Sci* 124:261–269. <http://dx.doi.org/10.1242/jcs.071928>.
 106. Rahimzadeh J, Meng F, Sachs F, Wang J, Verma D, Hua SZ. 2011. Real-time observation of flow-induced cytoskeletal stress in living cells. *Am J Physiol Cell Physiol* 301:C646–C652. <http://dx.doi.org/10.1152/ajpcell.00099.2011>.
 107. Ye N, Verma D, Meng F, Davidson MW, Suffoletto K, Hua SZ. 2014. Direct observation of α -actinin tension and recruitment at focal adhesions during contact growth. *Exp Cell Res* 327:57–67. <http://dx.doi.org/10.1016/j.yexcr.2014.07.026>.
 108. Meng F, Sachs F. 2012. Orientation-based FRET sensor for real-time

- imaging of cellular forces. *J Cell Sci* 125:743–750. <http://dx.doi.org/10.1242/jcs.093104>.
109. Iwai S, Uyeda TQP. 2008. Visualizing myosin–actin interaction with a genetically-encoded fluorescent strain sensor. *Proc Natl Acad Sci U S A* 105:16882–16887. <http://dx.doi.org/10.1073/pnas.0805513105>.
 110. De Angelis DA, Miesenböck G, Zemelmann BV, Rothman JE. 1998. PRIM: proximity imaging of green fluorescent protein-tagged polypeptides. *Proc Natl Acad Sci U S A* 95:12312–12316. <http://dx.doi.org/10.1073/pnas.95.21.12312>.
 111. Iwai S, Uyeda TQP. 2010. Myosin–actin interaction in Dictyostelium cells revealed by GFP-based strain sensor and validated linear spectral unmixing. *Cytometry A* 77:743–750. <http://dx.doi.org/10.1002/cyto.a.20900>.
 112. Borghi N, Sorokina M, Shcherbakova OG, Weis WI, Pruitt BL, Nelson WJ, Dunn AR. 2012. E-cadherin is under constitutive actomyosin-generated tension that is increased at cell–cell contacts upon externally applied stretch. *Proc Natl Acad Sci U S A* 109:12568–12573. <http://dx.doi.org/10.1073/pnas.1204390109>.
 113. Cai D, Chen S-C, Prasad M, He L, Wang X, Choesmel-Cadamuro V, Sawyer JK, Danuser G, Montell DJ. 2014. Mechanical feedback through E-cadherin promotes direction sensing during collective cell migration. *Cell* 157:1146–1159. <http://dx.doi.org/10.1016/j.cell.2014.03.045>.
 114. Conway DE, Breckenridge MT, Hinde E, Gratton E, Chen CS, Schwartz MA. 2013. Fluid shear stress on endothelial cells modulates mechanical tension across VE-cadherin and PECAM-1. *Curr Biol* 23:1024–1030. <http://dx.doi.org/10.1016/j.cub.2013.04.049>.
 115. Krieg M, Dunn AR, Goodman MB. 2014. Mechanical control of the sense of touch by β -spectrin. *Nat Cell Biol* 16:224–232. <http://dx.doi.org/10.1038/ncb2915>.
 116. Paszek MJ, DuFort CC, Rossier O, Bainer R, Mouw JK, Godula K, Hudak JE, Lakins JN, Wijekoon AC, Cassereau L, Rubashkin MG, Magbanua MJ, Thorn KS, Davidson MW, Rugo HS, Park JW, Hammer DA, Giannone G, Bertozzi CR, Weaver VM. 2014. The cancer glycocalyx mechanically primes integrin-mediated growth and survival. *Nature* 511:319–325. <http://dx.doi.org/10.1038/nature13535>.
 117. Stabley DR, Jurchenko C, Marshall SS, Salaita KS. 2012. Visualizing mechanical tension across membrane receptors with a fluorescent sensor. *Nat Methods* 9:64–67. <http://dx.doi.org/10.1038/nmeth.1747>.
 118. Morimatsu M, Mekhdjian AH, Adhikari AS, Dunn AR. 2013. Molecular tension sensors report forces generated by single integrin molecules in living cells. *Nano Lett* 13:3985–3989. <http://dx.doi.org/10.1021/nl4005145>.
 119. Green NM. 1990. Avidin and streptavidin. *Methods Enzymol* 184:51–67.
 120. Pfaff M, Tangemann K, Muller B, Gurrath M, Muller G, Kessler H, Timpl R, Engel J. 1994. Selective recognition of cyclic RGD peptides of NMR defined conformation by α II β 3, α V β 3, and α 5 β 1 integrins. *J Biol Chem* 269:20233–20238.
 121. Englund EA, Wang D, Fujigaki H, Sakai H, Micklitsch CM, Ghirlando R, Martin-Manso G, Pendrak ML, Robers DD, Durell SR, Appella DH. 2012. Programmable multivalent display of receptor ligands using peptide nucleic acid nanoscaffolds. *Nat Commun* 3:614. <http://dx.doi.org/10.1038/ncomms1629>.
 122. Jamali Y, Jamali T, Mofrad RRK. 2013. An agent based model of integrin clustering: exploring the role of ligand clustering, integrin homo-oligomerization, integrin–ligand affinity, membrane crowdedness and ligand mobility. *J Comp Phys* 244:264–278. <http://dx.doi.org/10.1016/j.jcp.2012.09.010>.
 123. Deng L, Kitova EN, Klassen JS. 2013. Dissociation kinetics of the streptavidin–biotin interaction measured using direct electrospray ionization mass spectrometry analysis. *J Am Mass Spectrom* 24:49–56. <http://dx.doi.org/10.1007/s13361-012-0533-5>.
 124. Klumb LA, Chu V, Stayton PS. 1998. Energetic roles of hydrogen bonds at the ureido oxygen binding pocket in the streptavidin–biotin complex. *Biochemistry* 37:7657–7663. <http://dx.doi.org/10.1021/bi9803123>.
 125. Tabard-Cossa V, Wiggan M, Trivedi D, Jetha NN, Dwyer JR, Marziali A. 2009. Single-molecule bonds characterized by solid-state nanopore force spectroscopy. *ACS Nano* 3:3009–3014. <http://dx.doi.org/10.1021/nn900713a>.
 126. Liu Y, Yehl K, Narui Y, Salaita K. 2013. Tension sensing nanoparticles for mechano-imaging at the living/nonliving interface. *J Am Chem Soc* 135:5320–5323. <http://dx.doi.org/10.1021/ja401494e>.
 127. Liu Y, Medda R, Liu Z, Galior K, Yehl K, Spatz JP, Cavalcanti-Adam EA, Salaita K. 2014. Nanoparticle tension probes patterned at the nano-scale: impact of integrin clustering on force transmission. *Nano Lett* 14:5539–5546. <http://dx.doi.org/10.1021/nl501912g>.
 128. Yun CS, Javier A, Jennings T, Fisher M, Hira S, Peterson S, Hopkins B, Reich NO, Strouse GF. 2005. Nanometal surface energy transfer in optical rulers, breaking the FRET barrier. *J Am Chem Soc* 127:3115–3119. <http://dx.doi.org/10.1021/ja043940i>.
 129. Zhang Y, Ge C, Zhu C, Salaita K. 2014. DNA-based digital tension probes reveal integrin forces during early cell adhesion. *Nat Commun* 5:5167. <http://dx.doi.org/10.1038/ncomms6167>.
 130. Blakely BL, Dumelin CE, Trappman B, McGregor LM, Choi CK, Anthony PC, Duesterberg VK, Baker BM, Block SM, Liu DR, Chen CS. 2014. A DNA-based molecular probe for optically reporting cellular traction forces. *Nat Methods* 11:1229–1232. <http://dx.doi.org/10.1038/nmeth.3145>.
 131. Wang X, Ha T. 2013. Defining single molecular forces required to activate integrin and Notch signaling. *Science* 340:991–994. <http://dx.doi.org/10.1126/science.1231041>.
 132. Huang B, Bates M, Zhuang X. 2009. Super resolution fluorescence microscopy. *Annu Rev Biochem* 78:993–1016. <http://dx.doi.org/10.1146/annurev.biochem.77.061906.092014>.
 133. Schermelleh L, Heintzmann R, Leonhardt H. 2010. A guide to super-resolution fluorescence microscopy. *J Cell Biol* 190:165–175. <http://dx.doi.org/10.1083/jcb.201002018>.
 134. Kanchanawong P, Shtengel G, Pasapera AM, Ramko EB, Davidson MW, Hess HF, Waterman CM. 2010. Nanoscale architecture of integrin-based cell adhesions. *Nature* 468:580–586. <http://dx.doi.org/10.1038/nature09621>.
 135. Morimatsu M, Mekhdjian AH, Chang AC, Tan SJ, Dunn AR. 2015. Visualizing the interior architecture of focal adhesions with high-resolution traction maps. *Nano Lett* 15:2220–2228. <http://dx.doi.org/10.1021/nl5047335>.
 136. Zimmerman T, Rietdorf J, Pepperkok R. 2003. Spectral imaging and its application in live cell microscopy. *FEBS J* 274:87–92. [http://dx.doi.org/10.1016/S0014-5793\(03\)00521-0](http://dx.doi.org/10.1016/S0014-5793(03)00521-0).
 137. Gordon WR, Vardar-Ulu D, Histén G, Sanchez-Irizarry C, Aster JC, Blacklow SC. 2007. Structural basis for autoinhibition of Notch. *Nat Struct Mol Biol* 14:295–300. <http://dx.doi.org/10.1038/nsmb1227>.
 138. Stephenson NL, Avis JM. 2012. Direct observation of proteolytic cleavage at the S2 site upon forced unfolding of the Notch negative regulatory region. *Proc Natl Acad Sci U S A* 109:E2757–E2765. <http://dx.doi.org/10.1073/pnas.1205788109>.
 139. Meloty-Kapella L, Shergill B, Kuon J, Botvinick E, Weinmaster G. 2012. Notch ligand endocytosis generates mechanical pulling force dependent on dynamin, epsins, and actin. *Dev Cell* 22:1299–1312. <http://dx.doi.org/10.1016/j.devcel.2012.04.005>.
 140. Reference deleted.
 141. Sun X, Artavanis-Tsakonas S. 1997. Secreted forms of DELTA and SERRATE define antagonists of Notch signaling in *Drosophila*. *Development* 124:3439–3448.
 142. Narui Y, Salaita K. 2013. Membrane tethered Delta activates Notch and reveals a role for spatio-mechanical regulation of the signaling pathway. *Biophys J* 105:2655–2665. <http://dx.doi.org/10.1016/j.bpj.2013.11.012>.
 143. Hicks C, Ladi E, Lindsell C, Hsieh JJ-D, Hayward SD, Collazo A, Weinmaster G. 2002. A secreted Delta1-Fc fusion protein functions both as an activator and inhibitor of Notch1 signaling. *J Neurosci Res* 68:655–667. <http://dx.doi.org/10.1002/jnr.10263>.
 144. Perez-Jimenez R, Alonso-Caballero A, Berkovich R, Franco D, Chen M-W, Richard P, Badilla CL, Fernandez JM. 2014. Probing the effect of force on HIV-1 receptor CD4. *ACS Nano* 8:10313–10320. <http://dx.doi.org/10.1021/nn503557w>.